Mixing Improvement by Manipulation of Multiple Jets Using Active Plasma Actuator

N. Benard[1], A. Mizuno[2], and E. Moreau[1]
[1]Institut PPRIME (CNRS UPR 3346, University of Poitiers, ISAE-ENSMA), France
[2]Department of Environmental and Life Sciences, Toyohashi University of Technology, Japan

Abstract—This study interests in defining a new type of dielectric barrier discharge actuator for mixing improvement purpose. The actuator is composed of a perforated plate (121 holes) housing embedded and printed electrodes between which a high voltage is applied. The electrode arrangement is such that the holes where the gas flows are surrounded by dielectric barrier discharges. Electrical and optical characterizations of the discharge are proposed to characterize the typical streamer and glow regimes that occur during one period of the AC sine voltage. Fast flow imaging by smoke streamwise and cross-sectional visualizations has been conducted for a freestream flow of 5 m/s. Depending on the applied frequency, the plasma discharge can modify the outer region where secondary instability takes place or it can produce a laminar-to-turbulent transition, enhancing then the mixing of the flow exiting from the perforated plate.

Keywords—Plasma actuator, dielectric barrier discharge, jet flow, flow control

I. Introduction

The mixing of scalar flow component is important for a large number of practical and fundamental situations. Mixing by passively forced turbulence underlies a variety of engineering phenomena, including combustion, injection cooling, industrial mixing and pollution transport. Turbulent mixing can also be viewed from a fundamental point of view by theoretical and empirical methods. For instance, the decay of turbulent components in grid-generated turbulence, where homogeneous and isotropic turbulence quickly develops, is intensively studied since many years now [1], [2]. A few systems have been designed to modify the obvious power-law decay of the turbulent components. One can mention the fractal grids developed by Vassilicos et al. that produce better mean flow homogeneity and a high turbulent intensity while maintaining a low pressure drop [3], [4]. The turbulence characteristics can also be improved considerably by employing multiple grids in series as it was shown in Mazellier et al. [5], [6]. Nonetheless, most of these systems improving the turbulent characteristics are passive devices. Only a few active control systems for grid turbulence have been developed [7]. The primary limitation of these active systems is that, despite of providing an effective control of the turbulent characteristics, these mechanical systems are extremely complex. Furthermore, the use of a mechanical system means that only low frequency excitation can be applied. This is a strong limitation if one attempts at promoting flow structures of many different sizes, from short to long wavelengths that would interact by multiscale dynamics and energy exchanges. Another method for increasing the mixing of turbulent flow is the use of multiple jets for which considerable investigations have been conducted in research related to combustion or chemical mixing. For example, a fuel jet can be confined by lateral oxygen jets in order to stabilize a flame by increasing the surrounding mixing, this stabilization leading to a significant reduction of pollutant emissions such as NOx [8]. Multi-jet burners are effective designs to improve combustion intensity and shorten the length of the flame [9], but multiple interacting jets produce complex flows and have not been thoroughly investigated. For instance, the near-field behavior of 6×6 interacting jets has been recently investigated by mean of PIV and LDA measurements [10]. The merging of the jets into a single jet after a certain distance has been confirmed. A deflection of peripheral jets towards the center of the jet array is also reported; the deflection being caused by mutual entrainment between the jets and a low pressure region at the center of the jet array.

The present paper proposes to define and demonstrate that surface plasma discharges can be useful for mixing increase in the wake of an active “grid like” or “multi-jet like” geometry. The use of non-thermal surface plasma discharge for flow control is now more than an emerging field. More than fifteen years of investigations [11]–[13] have demonstrated the benefits of plasma actuators in a large number of flow conditions, including separated turbulent flow caused by pressure gradient or geometric accident [14]–[16], plane and axisymmetric mixing layers [17], [18], aerofoil and landing gear noise production [19], [20] and so many more specific applications. Plasma-assisted flow control is now a well-established research domain, involving more and more research groups but the typical surface plasma actuator with asymmetric electrodes, as it was originally defined by Roth [21], is still the most used configuration. The present paper aims at investigating a different type of electrode arrangement installed on a perforated flat plate in order to tackle new applicative and fundamental problems dedicated to mixing enhancement. This type of complex electrode arrangement has been originally designed for gas cleaning by combination of non-thermal plasma and catalysts (named as honeycomb

Corresponding author: Nicolas Benard
e-mail address: Nicolas.benard@univ-poitiers.fr

Presented at the 3rd ISNPEDADM 2015 (New electrical technologies for environment), in October 2015

plasma discharge in [22]), but plasma grids have also been investigated for air decontamination in [23] and [24] among many references from the same authors. In the first parts of this paper, electrical and optical diagnostic are proposed in order to characterize the honeycomb plasma discharge. Then, the mean airflow downstream of the perforated plate is visualized in absence and in presence of the plasma discharge operated at different electrical conditions. The primary objective is to identify if this innovative plasma actuator can manipulate a gas flow. An active manipulation of the wake of the plate means that the system will be useful for multi-jet burners. Indeed, such active system can take advantages of the high frequency forcing capability of plasma discharges in order to increase the turbulent motion at the smallest scales where immediate effect on chemical reactions that occur on the molecular level could be observed.

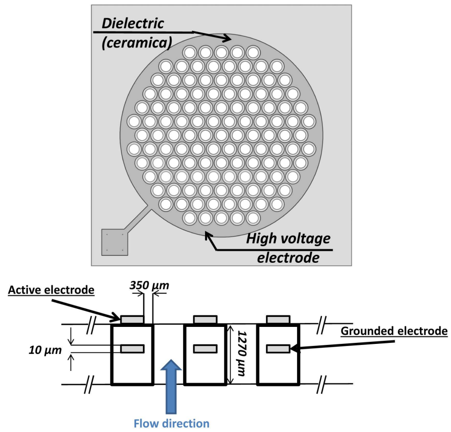

Fig. 1. Sketch (front and slice views) of the honeycomb plasma actuator.

II. Methodology

A. Geometry of the honeycomb plasma actuator

The plasma actuator is made of a ceramic plate (Al_2O_3, 92% with a thickness of 1.27 mm) perforated by 121 holes having an inner diameter, Φ, of 2 mm (Fig. 1). The top of the plasma actuator is made of a conductive layer (nickel with thickness of 10 μm) connected to a high-voltage power supply. The grounded electrode is embedded within the ceramic dielectric material at a distance of 630 μm from the air-exposed electrode. The distance between the edge of an active electrode and the edge of the corresponding hole designed for the gas passage is 350 μm (see Fig. 1). The distance between the centers of two successive holes is 3.05 mm. At a sufficient onset voltage, the plasma discharge array is fully powered (see Fig. 2), the electric field producing a visible discharge around each of the holes (at the surface, but also inside the lateral edge of the holes).

B. Electrical setup

A sinusoidal waveform is generated by a function generator (Hameg, 8110). A signal amplifier (Trek, model 30 kV-40 mA) is used to apply a gain of 3000 V/V to the input voltage. The applied voltage amplitude reaches maximum value up to 14 $kV_{p\text{-}p}$ while the AC frequency driving the plasma formation ranges from 100 up to 2000 Hz. Measurements of the total current discharge are conducted by measuring the voltage across a non-inductive shunt resistor (100 Ω) connected to the grounded electrode. Electrical measurements also include calculation of the consumed electrical power by a capacitor-based charge method (MKP 47 nF 630 V capacitor). The total current signal and charge is digitized by a high-resolution oscilloscope (Lecroy, HDO 6054).

C. Optical diagnostic

The plasma layer developing at the dielectric surface is recorded by a fast gateable EM-iCCD camera (Princeton, Pi-max4 Gen2) with 1024×1024 pixel^2 matrix. The camera is equipped with a 200 mm objective coupled to a focal length doubler in order to reach a magnification scale of 1:1 (field of view of 9×9 mm^2).

The present paper aims at demonstrating the capabilities of the honeycomb plasma discharge for increasing the turbulent transfer of a flow passing through its holes. In order to characterize the flow modifications imposed by the discharge, smoke flow visualizations have been performed using a short-pulsed Nd:YLF laser (Terra PIV 527-100-M) that generates a visible green light ($\lambda = 527$ nm) and delivers 30 mJ per oscillator when operated at 1 kHz. This equipment is used for visualizing the instantaneous flow field (exposure time of about 100 μs) and the flow structures embedded in the background turbulence if they exist. A fast camera (Photron SA-Z) is synchronized with the laser for operating the optical diagnostic at 1300 Hz. This sampling rate differs from the applied f_{AC} in order to avoid any phase-averaging bias. The laser sheet is placed perpendicularly in the central axis of the honeycomb to visualize the flow along its convection in the streamwise direction. Cross-sectional smoke visualizations are also proposed at a distance of 10.8 mm from the honeycomb actuator. Dielectric oil (Ondina 15) is atomized into fine droplets for permitting the laser light scattering. For each of the tests, a flow sequence of 5000 images has been recorded. The raw images are processed using Davis 8.2 software. Each of these images is normalized by subtracting the minimal intensity value of the whole image. Finally, for a time-averaged description of the flow field, the mean grey level of the 5000 images is computed.

D. Flow conditions

The honeycomb plasma discharge has been implemented at the exhaust of a circular open-air type wind-tunnel with a 0.132 m^2 cross-section. This facility has a 1.45 m long chamber, series of mesh grids and a jet exit of 50 mm in diameter is obtained by means of a contraction outlet which improves the flow uniformity (contraction ratio of 1:17). The air flow is driven by a centrifugal fan (FEVI F18G-1R-500, France) with eight radial blades rotating at a maximum rpm of 3,000 delivering 0.3 m^3/s. The local velocity (U_0), measured at the center of one hole of the plasma actuator array, is fixed

Fig. 2. Photographs of the plasma discharge array prototype (left), mounted at the jet exhaust (center) and powered by an AC voltage with amplitude of 14 kV$_{p\text{-}p}$ at 2000 Hz (right).

at 5 m/s (Reynolds numbers of $\mathrm{Re}_\Phi = 985$). At such a low Reynolds number, the jets are initially in a laminar regime but they can become rapidly unstable and turbulent eddies can form at some distance away from the outlet of the honeycomb discharge.

III. Results

A. Electrical results

Typical traces of voltage and current time evolutions are illustrated in Figs. 3 and 4 for different voltages (with f_{AC} fixed at 2000 Hz) and frequencies (for applied voltage amplitude of 14 kV$_{p\text{-}p}$), respectively. The plots in both figures clearly show that the plasma discharge array mostly behaves as a typical dielectric barrier discharge. Indeed, two plasma regimes can be inferred from the total current measurement, these two regimes being superimposed on a strong capacitive signature caused by the electrode arrangement of the device. One can recognize a streamer regime made of numerous positive current peaks during the positive-going cycle of the voltage signal. The number and amplitude of these peaks increases with the applied voltage (Fig. 3) and the applied AC frequency (Fig. 4). For the higher consumed power (15 W), the current peaks reach amplitude up to 80 mA. Increasing the applied voltage enhances the duration of the streamer regime (the streamer regime starts earlier with an increasing voltage) when applying a higher driven frequency has almost no influence on the duration of the regime. As it is shown in Figs. 3 and 4, the negative-going cycle of the voltage results in small amplitude negative current peaks (~5 mA). The plasma discharge corresponds then to a glow regime whose intensity can be increased by a higher voltage amplitude and f_{AC}. The increase in current amplitudes (both positive and negative) suggests a higher electrical power consumed by the actuator. The electrical power consumption measurements are gathered in Fig. 5. The measurements indicate a maximum consumed power of 15 W for the whole system, but lowered electrical power consumption can be achieved by reducing the applied voltage amplitude and/or AC frequency. The rate of increase in the consumed power is higher with an increasing voltage (quadratic increase) than with an increasing frequency (linear increase). One can notice that the onset voltage for the plasma actuator array is of about 4 kV$_{p\text{-}p}$, the exact value depending on the applied frequency (it decreases with f_{AC}).

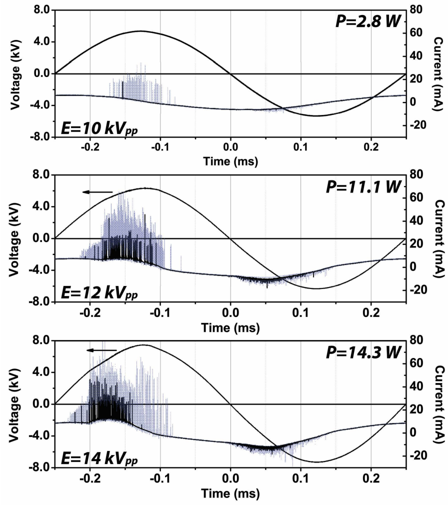

Fig. 3. Total measured current for varying voltage amplitudes ($f_{AC} = 2000$ Hz). The instantaneous snapshot of one AC cycle is plotted in black and the envelope of 200 AC cycles is shown in blue.

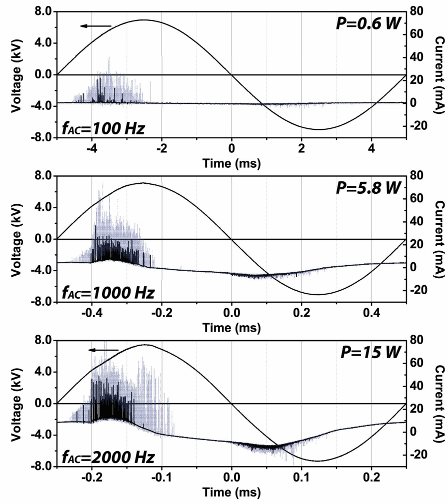

Fig. 4. Total measured current for varying driven AC frequencies f_{AC} (14 kV$_{p\text{-}p}$).

B. Morphology of the discharge by ICCD

This section interests in characterizing the plasma discharge by top-view EM-iCCD visualizations. By using a short expo-

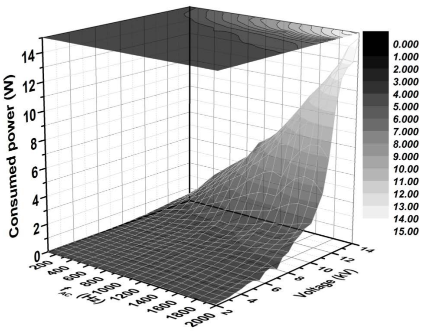

Fig. 5. Electrical power consumed by the honeycomb plasma discharge.

sure time with a well-chosen duration, both plasma regimes can be discriminated. In Fig. 6 is shown the plasma morphology for varying f_{AC} while the voltage amplitude is fixed at 14 kV$_{p\text{-}p}$. As it was observed in the previous section, the current discharge is clearly affected when f_{AC} is increased but the images of the ionized regions are not fundamentally changed. The positive-going cycle of the voltage signal corresponds to a corona-like discharge covering the distance from the active electrode edges to the border of the holes but strong light emission is also produced by some intense spots (streamer), this being responsible for the high amplitude positive current peaks. It seems that only one streamer occurs per hole of the honeycomb DBD discharge. The morphology of the discharge differs for the negative-going cycle of the voltage. In this case, the current trace evokes a glow regime with many filaments propagating at the dielectric surface. They connect the edge of the active electrode to the border of the hole, several of them being observed per hole. However, the intensity of these filaments is three times lower than the light emitted by the streamers. An increase in frequency reinforces the intensity of the streamer, but the global aspect of the streamer regime is not strongly modified. The influence of f_{AC} on the glow regime is even less discernible. The only modification is a small increase in the light emitted by the ionized filaments.

A similar experiment has been conducted for a f_{AC} maintained constant at 2000 Hz and voltage amplitude of 10 and 14 kV$_{p\text{-}p}$ (Fig. 7). As for the changes in plasma morphology with f_{AC}, the voltage amplitude has a strong influence on the streamer regime, but the glow regime seems mostly insensitive. At the lowest voltage amplitude, only a few streamers are formed during the positive-going cycle of the voltage but low density ionization occurs over the dielectric surface. As already indicated, the voltage amplitude has almost no influence on the morphology of the glow regime.

C. Flow modifications imposed by the plasma actuator

Streamwise view of the flow in absence of plasma discharge can be viewed in Fig. 8 (natural flow case). These streamwise visualizations show the traces of the jets issuing from all the holes of the honeycomb discharge. As in [10], the peripheral jets are rapidly deflected toward the axis of the wake flow due to the mutual interactions of the jets and to the low pressure region at the center of the wake. The present measurements indicate that the multi-jet quickly evolves as a single jet with a potential core surrounded by convected ring vortices at the origin of the axisymmetric shear layer.

The flow topology by cross-sectional images is shown in Fig. 9, this plot highlighting the symmetry of the flow in the initial region. Each of the single jets issuing from the holes of the honeycomb discharge is clearly observed in the cross-sectional view, but they are not aligned with their originating hole due to the peripheral deflection already reported from the streamwise images. The single jets in the outer boundary region of the global jet quickly lose their coherency and the initial round jets rapidly evolve into mushroom-like vortices.

The structuration of the outer boundary region resembles the streamwise vortex pairs many times reported in literature for a single round laminar jet [25], [26]. In round jet configuration, the streamwise vortex pairs (secondary instability) originate from the interactions of successive ring structures formed at the jet periphery (primary instability), but here there is no clear signature of a primary instability in the cross-sectional images. One can suspect that the peripheral flow structures are formed under the shearing force caused by the large local velocity gradient between the air jet and the surrounding quiescent flow. For the single jets issuing from the holes located in the central region of the honeycomb discharge, they lose their round aspects and are deformed to finally approach a square shape. Indeed, the mutual interaction between adjacent jets changes the flow conditions in the boundary region of each jet by comparison with a single jet exiting in a quiescent environment. Finally, in the present configuration, each of the jet is in a situation of coflow. The topology of the jets in the central region resembles to the helicoid mode 4 observed in [27] where coaxial jets with a swirling movement of the outer jet were studied.

The cases of flow forced by the plasma discharge are also depicted in Figs. 8 and 9. For a f_{AC} frequency equal to 100 Hz, the influence of the discharge on the mean flow is limited to the boundary region of the global jet. In the streamwise view (Fig. 8), the influence of the discharge corresponds to a higher deflection of the peripheral jets, finally resulting in a shortening of the region where the multiple jets interact. As it is shown in the central plot of Fig. 9, the symmetry and the topology of the cross-sectional image is not fundamentally modified, but the periodic perturbations imposed by the discharge have sufficient amplitude to partially break the mean vortical flow organization of the outer region while the inner region of the jet remains unchanged. By increasing further the f_{AC} value, the region of jet interaction is reduced further. As shown in the cross-sectional view, the structuration of the flow is fully modified without any signature of flow organization at large-scale and it corresponds now to a fully turbulent flow regime at the measurement location. Here, the flow visualizations suggest that the mixing process is enhanced by the plasma discharge due to a forced laminar-to-turbulent transition, a turbulent flow being intimately connected with a higher mixing capability.

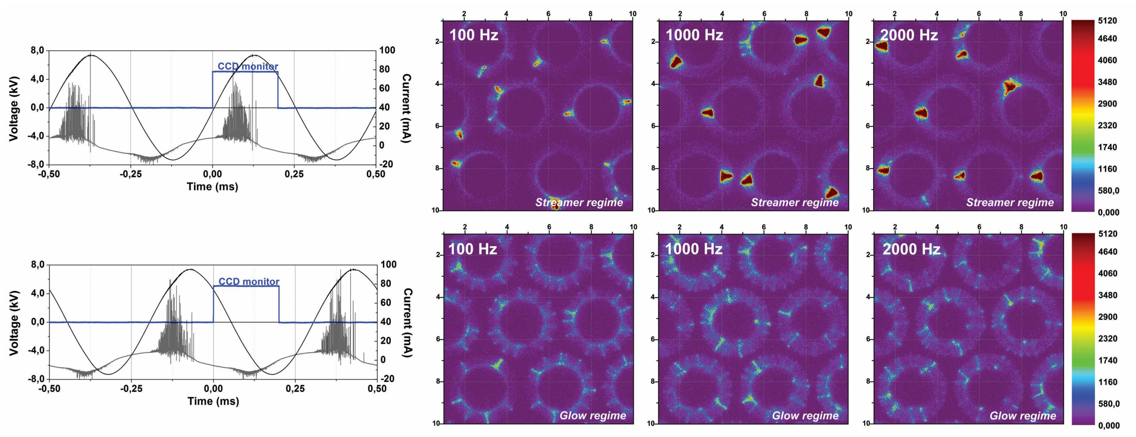

Fig. 6. Visualizations with short exposure time for varying f_{AC} (the two plasma regimes are discriminated).

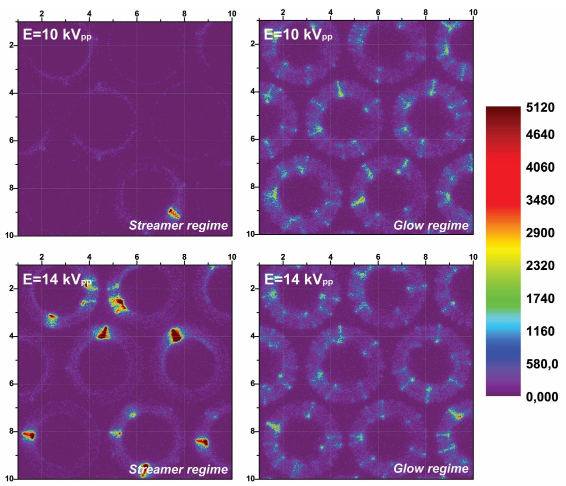

Fig. 7. Comparison of the plasma morphology for the two extrema of the applied voltage amplitude.

IV. Conclusion

The present paper investigates the use of a novel type of dielectric barrier discharge for jet flow control. The direct application relates to mixing enhancement in combustion in order to gain a better efficiency of combustion and thus a reduction of pollutant formation. The electrical measurements have confirmed that the electrode geometry leads to the formation of a typical surface plasma discharge in presence of a dielectric barrier. The two plasma regimes, namely the streamer and glow regimes, have been observed from the time evolution of the current and from short-exposure time images of the plasma layer. In situation of flow control, the conducted experiments reveal the potential of this discharge in term of mixing improvement. According to the flow conditions, the jets at the outlet of the holes are initially in a laminar regime, but the plasma discharge can actively force a turbulent flow regime in the wake of the plasma array, providing that the applied AC frequency is large enough. Here, the mixing enhancement of the multi-jet with the ambient air is achieved by a transition from a laminar regime to a turbulent one when f_{AC} is equal to 2000 Hz. Knowing that this system is effective to manipulate a laminar flow, additional measurements will be conducted to characterize the influence of the plasma discharge for jet flow in an initially turbulent regime. These measurements should include high-resolution PIV and time-resolved analysis to address the capability of this original discharge for manipulating the isotropic character of the turbulent flow field, the Reynold stress components, the integral length scales or the decay law along the centerline of the global jet formed in the wake of the honeycomb plasma discharge.

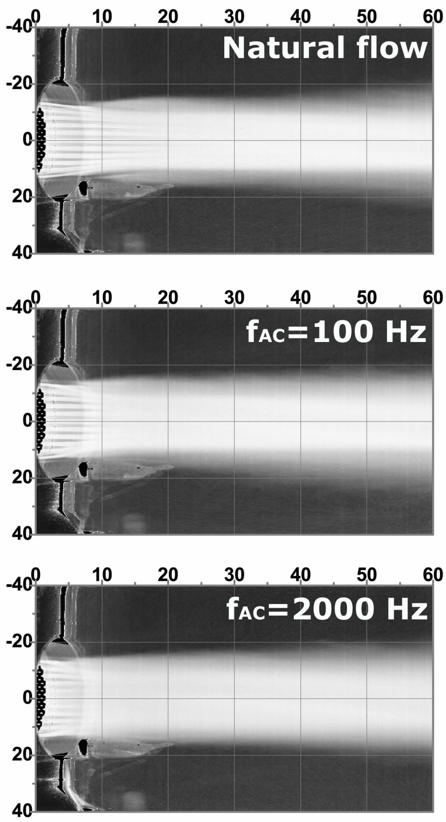

Fig. 8. Streamwise smoke visualizations of the flow for unforced and forced conditions (dimensions in mm).

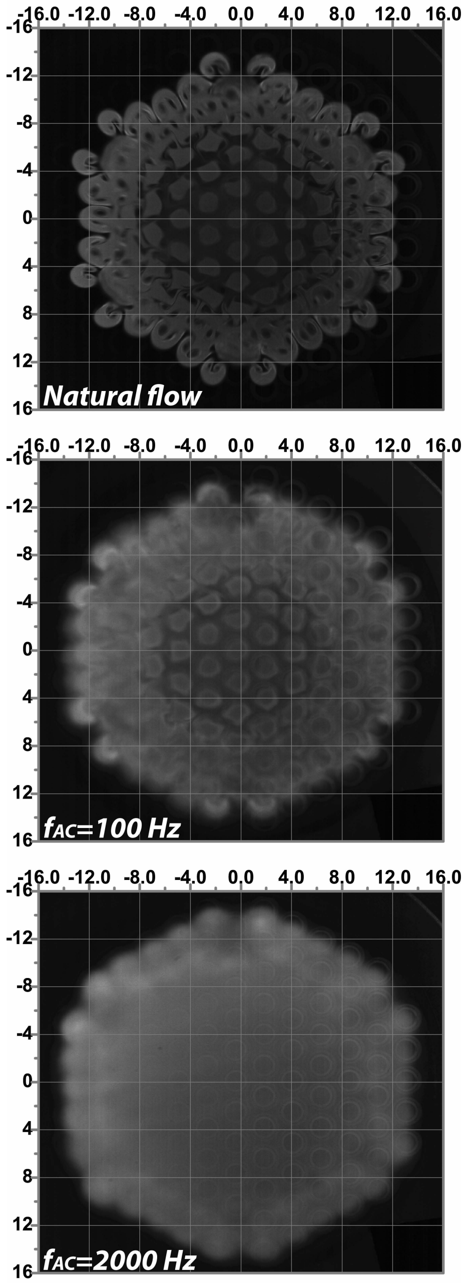

Fig. 9. Cross-sectional smoke visualizations of the flow for unforced and forced conditions (dimensions in mm).

ACKNOWLEDGMENT

The equipment used in this work was funded by the French Government program “Investissements dAvenir” (LABEX INTERACTIFS, reference ANR-11-LABX-0017-01). This work is conducted under DGA supervision and partially funded by ANR (INOPLAS, ANR-13-ASTR-0015-01).

This work was partly supported by a Grant-in-Aid for Scientific Research (KAKENHI 24108005) from the Ministry of Education, Culture, Sports, Science and Technology (MEXT), Japan. The authors are also grateful for Kyocera Co.

REFERENCES

[1] G. Comte-Bellot and S. Corrsin, “Simple eulerian time correlation of full-and narrow-band velocity signals in grid-generated, isotropic turbulence,” *Journal of Fluid Mechanics*, vol. 48, pp. 273–337, 1971.

[2] P. E. Roach, “The generation of nearly isotropic turbulence by means of grids,” *International Journal of Heat and Fluid Flow*, vol. 8, pp. 82–92, 1987.

[3] R. Gomes-Fernandes, B. Ganapathisubramani, and J. C. Vassilicos, “Particle image velocimetry study of fractal-generated turbulence,” *Journal of Fluid Mechanics*, vol. 711, pp. 306–336, 2012.

[4] S. Laizet and J. C. Vassilicos, “DNS of fractal-generated turbulence,” *Flow, Turbulence and Combustion*, vol. 87, pp. 673–705, 2011.

[5] N. Mazellier, L. Danaila, and B. Renou, “Multi-scale energy injection: A new tool to generate intense homogeneous and isotropic turbulence for premixed combustion,” *Journal of Turbulence*, vol. 11, pp. 1–30, 2010.

[6] R. Fragner, N. Mazellier, F. Halter, C. Chauveau, and I. Gökalp, “Multi-scale high intensity turbulence generator applied to a high pressure turbulent burner,” *Flow, Turbulence and Combustion*, vol. 94, pp. 263–283, 2014.

[7] H. S. Kang, S. Chester, and C. Meneveau, “Decaying turbulence in an active-grid-generated flow and comparisons with large-eddy simulation,” *Journal of Fluid Mechanics*, pp. 129–160, 2003.

[8] T. Boushaki, M. A. Mergheni, J. C. Sautet, and B. Labegorre, “Effects of inclined jets on turbulent oxy-flame characteristics in a triple jet burner,” *Experimental Thermal and Fluid Science*, vol. 32, pp. 1363–1370, 2008.

[9] Q. F. Liang, Q. H. Guo, G. S. Yu, and F. C. Wang, “An experimental investigation on characteristics of individual flame and multi-jet flame,” *Energy Sources, Part A: Recovery, Utilization and Environmental Effects*, vol. 35, pp. 1476–1485, 2013.

[10] S. Ghahremanian, K. Svensson, M. J. Tummers, and B. Moshfegh, “Near-field development of a row of round jets at low reynolds numbers,” *Experiments in Fluids*, vol. 55, 2014.

[11] T. C. Corke, C. L. Enloe, and S. P. Wilkinson, “Dielectric barrier discharge plasma actuators for flow control,” *Annual Review of Fluid Mechanics*, vol. 42, pp. 505–529, 2010.

[12] J.-J. Wang, K.-S. Choi, L.-H. Feng, T. N. Jukes, and R. D. Whalley, “Recent developments in DBD plasma flow control,” *Progress in Aerospace Sciences*, vol. 62, pp. 52 – 78, 2013.

[13] N. Benard and E. Moreau, “Electrical and mechanical characteristics of surface AC dielectric barrier discharge plasma actuators applied to airflow control,” *Experiments in Fluids*, vol. 55, 2014.

[14] T. C. Corke, M. L. Post, and D. M. Orlov, “Single-dielectric barrier discharge plasma enhanced aerodynamics: Concepts, optimization, and applications,” *Journal of Propulsion and Power*, vol. 24, pp. 935–945, 2008.

[15] N. Benard, J. Jolibois, and E. Moreau, “Lift and drag performances of an axisymmetric airfoil controlled by plasma actuator,” *Journal of Electrostatics*, vol. 67, pp. 133–139, 2009.

[16] P. Sujar-Garrido, N. Benard, E. Moreau, and J. P. Bonnet, “Dielectric barrier discharge plasma actuator to control turbulent flow downstream of a backward-facing step,” *Experiments in Fluids*, vol. 56, 2015.

[17] R. Ely and J. Little, “Mixing layer excitation by dielectric barrier discharge plasma actuators,” in *51st AIAA Aerospace Sciences Meeting including the New Horizons Forum and Aerospace Exposition 2013*, 2013.

[18] N. Benard, J. P. Bonnet, G. Touchard, and E. Moreau, “Flow control by dielectric barrier discharge actuators: Jet mixing enhancement,” *AIAA Journal*, vol. 46, pp. 2293–2305, 2008.

[19] F. O. Thomas, A. Kozlov, and T. C. Corke, “Plasma actuators for cylinder flow control and noise reduction,” *AIAA Journal*, vol. 46, pp. 1921–1931, 2008.

[20] X. Huang and X. Zhang, “Plasma actuators for noise control,” *International Journal of Aeroacoustics*, vol. 9, pp. 679–704, 2010.

[21] J. R. Roth, “Electrohydrodynamically induced airflow in a one atmosphere uniform glow discharge surface plasma,” in *1998 IEEE International on Plasma Science, 1998. 25th Anniversary.*, June 1998, pp. 291–.

[22] A. Mizuno, “Generation of non-thermal plasma combined with catalysts and their application in environmental technology,” *Catalysis Today*, vol. 211, pp. 2–8, 2013.

[23] K. Shimizu, “Indoor air control by microplasma,” in *Advanced air pollution*, F. Nejadkoorki, Ed. InTech, 2011, ch. 26, pp. 509–534.

[24] K. Shimizu, M. Blajan, and T. Kuwabara, "Removal of indoor air contaminant by atmospheric microplasma," *IEEE Transactions on Industry Applications*, vol. 47, pp. 2351–2358, 2011.

[25] D. Liepmann and M. Gharib, "The role of streamwise vorticity in the near-field entrainment of round jets," *Journal of Fluid Mechanics*, vol. 245, pp. 643–668, 1992.

[26] V. V. Kozlov, G. R. Grek, A. V. Dovgal, and Y. A. Litvinenko, "Stability of subsonic jet flows," *Journal of Flow Control, Measurement and Visualization*, vol. 1, pp. 94–101, 2013.

[27] T. Ivanic, E. Foucault, and J. Pecheux, "Dynamics of swirling jet flows," *Experiments in Fluids*, vol. 35, pp. 317–324, 2003.